PHYSICAL REVIEW C **79**, 044605 (2009)

Analytical potential for the elastic scattering of light halo nuclei below and close to the Coulomb barrier

L. Borowska,[1,2,*] K. Terenetsky,[2] V. Verbitsky,[2] and S. Fritzsche[3,4]
[1]*Universität Bonn, Auf dem Hügel 20, D-53121 Bonn, Germany*
[2]*Institute for Nuclear Research, National Academy of Sciences of Ukraine, Nauky Prospekt 47, 03680 Kyiv, Ukraine*
[3]*Gesellschaft für Schwerionenforschung (GSI), Planckstrasse 1, D-64291 Darmstadt, Germany*
[4]*Frankfurt Institute for Advanced Studies, D-60438 Frankfurt am Main, Germany*
(Received 7 December 2008; published 14 April 2009)

An analytical expression for the dynamic polarization potential is derived for the elastic scattering of light halo nuclei in the Coulomb field of heavy targets. The derivation is based on the adiabatic motion of the projectile below and close to the Coulomb barrier together with a uniform approximation for the Coulomb functions. Detailed computations have been carried out for the elastic scattering of $d + {}^{208}$Pb and ^{6}He + ^{208}Pb at collision energies of 8 and 17.8 MeV and are compared with measurements as far as available. The obtained expression for the dynamic polarization potential is simple and can be applied for any arbitrary system with a dineutron configuration.

DOI: 10.1103/PhysRevC.79.044605 PACS number(s): 21.60.−n, 24.70.+s, 25.60.Bx, 27.20.+n

I. INTRODUCTION

Light halo nuclei are exotic and weakly bound systems that have attracted a great deal of interest during the past decades. In particular, neutron-rich nuclei near the drip line provide a new path for studying nuclear matter and correlations at low densities. In these nuclei, the halo is often formed by one or several loosely attached (valence) neutrons with binding energies of less than 1 MeV and with low angular momenta ($l = 0, 1$). Because of their weak binding, the valence neutrons may extend far out in space and thus help us obtain information about the (range of) nuclear forces [1–3], neutron-neutron correlations [1,4–7], or even the (so-called) astrophysical S factors [8,9] that have been found useful to characterize nuclear reactions. Today, neutron halos are known not only for a number of light nuclei, such as ^{6}He, ^{11}Li, and ^{14}Be, but also for ^{19}C [1,4–6,8–12].

Nuclear scattering and transfer reactions are the main experimental techniques used to explore the neutron-neutron correlations and their interaction with the (more or less) inert core of the nuclei [1,13–15]. Apart from enhanced reaction cross sections for neutron transfer and some rather narrow momentum distributions of the reaction products, these measurements revealed sizable cross sections, especially for the elastic scattering and the Coulomb dissociation (breakup) of the halo nuclei in collisions with heavy targets below or close to the Coulomb barrier. To describe the anomalous behavior of these light (halo) nuclei, several semiclassical and quantum mechanical models have been developed that aim for a better understanding of the correlated motion of the neutrons and how this is affected by the properties of the nuclear core. In practice, however, a complete microscopic description has remained a great (theoretical and computational) challenge, and typically further approximations are required to deal with these reactions fully quantum mechanically. For this reason, it often appears more efficient to treat the neutron halo, the inert core, and the target as a *three-particle* system, within which all the (nuclear many-body) configurations of the halo nucleus are taken into account. The main theoretical method that follows this line is the continuum-discretized coupled channel theory (CDCC) [16,17] that has been developed recently. Apart from the discretization of the continuum of the projectiles, this method even enables one to treat the scattering of a three-body projectile in the field of the target as an “effective” four-body system [18,19].

From the viewpoint of semiclassical scattering theory, three techniques have been applied during the past decade to describe the electrical polarization as well as the Coulomb breakup of the neutron halo nuclei. These techniques include the coupled-channel approach [20], the adiabatic theory [10,21], and applications of some optical model potential [22]. In the semiclassical picture, the halo nucleus is hereby supposed to move along a classical (Rutherford) trajectory in the external Coulomb field of some heavy target. Emphasis in most previous work was placed especially on the elastic scattering of light halo nuclei to explore the structure and shape of the neutron halos. Much of the recent interest was focused moreover on finding an optical potential that would enable one to produce the elastic scattering cross sections in the strong electric field of heavy targets [15,23]. Although a number of case studies have been carried out for the Coulomb breakup and the near-barrier fusion cross section, based on the time-independent Schrödinger equation for the motion of the halo nucleus in the Coulomb field of heavy targets [20,23–25], less attention has been paid so far to improve the optical potentials available for their elastic scattering.

A first attempt to obtain a dynamic polarization potential (DPP) was made some years ago by Andres *et al.* [22], who applied the semiclassical Coulomb excitation amplitudes to calculate the scattering of ^{11}Li on ^{208}Pb nuclei at energies around and above the Coulomb barrier (26 MeV). It should be noted however that, in their approach, the real polarization potential was obtained from the behavior of the imaginary

*borowska@uni-bonn.de

potential at the given projectile energy and as function of the dipole excitation energy. Therefore, the polarization potential was quite sensitive with regard to uncertainties in the distribution of the dipole strength. More recently Sanchez-Benitez *et al.* [14] have described the scattering of ^{6}He on ^{208}Pb nuclei at energies around the Coulomb barrier by using the prescription developed in Ref. [22]. To reproduce the experimental data, however, a very large (so-called) diffuseness parameter a_i (2.21 fm) was needed for the imaginary part of the potential, which appears to be rather unusual. Later, Moro *et al.* [26] also applied the CDCC approach to describe the elastic scattering of ^{6}He. In that work, the $^6\text{He} + {}^{208}\text{Pb}$ interaction potential was obtained from the interactions between the dineutron and the target as well as the α-like core and the target, and this was folded with some internal function from the ^{6}He projectile. However, to make the rms point nucleon matter radius consistent with the value from the three-body calculation, they needed to set the two-neutron separation energy to a rather unrealistic value.

A different viewpoint in obtaining a DPP for the elastic scattering of light halo nuclei in the Coulomb field of heavy targets is taken by the *adiabatic* model, which was developed recently by us [21]. In this model, the internal motion of the halo nucleus is assumed to be fast when compared with its motion through the Coulomb field of the target. With this assumption in mind, we derived an implicit equation for the DPP that is independent of any parameter (other than it is required to describe the scattering process) and can be applied for the scattering of any dineutron configuration. So far, however, this implicit equation could not be solved analytically but had to be obtained numerically by using a quasiclassical approach. In the present work, an analytical expression for the DPP is derived in terms of the Airy functions. This expression is based on the adiabatic and the uniform approximations for the elastic scattering of light deuteron-like nuclei in the Coulomb field of heavy targets. In fact, this potential can be applied for any light and weekly bound system with a dineutron configuration and may be utilized also for light neutron halo nuclei.

The paper is organized as follows. In the next section, we shall start from the Schrödinger equation of the dineutron halo in the Coulomb field of the target and first divide this equations in two: one equation for the center-of-mass motion along the Rutherford trajectory and a second one for describing the internal motion of the halo nucleus (Sec. II A). From the "coupling" of these equations, an expression is then obtained for the DPP in Sec. II B by using the uniform approximation for the internal motion of the projectile. This analytical form of the polarization potential is later utilized in Sec. III to calculate the elastic angle-differential cross sections for the collision of low-energy ^{6}He ions with ^{209}Bi and ^{208}Pb targets. Good agreement is found with recent experiments [13,15]. Finally, a brief summary is given in Sec. IV.

II. THEORY

To describe the elastic scattering of neutron-halo nuclei in the Coulomb field of heavy targets below and close to the Coulomb barrier, let us assume for the projectile a *deuteron-like* structure in which the neutral halo ("neutron") with mass m_n revolves around the charged core ("proton") with mass m_p and charge Z_p. In this simplified picture, the total mass of the halo nucleus ("deuteron") is $m_d \simeq m_n + m_p$, while the (binding) energy needed to break the halo nucleus into its "proton" and "neutron" clusters is supposed to be

$$\varepsilon_0 = -\frac{\hbar^2\alpha^2}{2\mu},$$

with $\mu = m_n m_p/m_d$ being the reduced mass as associated with the relative motion of the neutron halo and the core. For the target, moreover, we shall assume in the following a heavy and (nearly) magic nucleus with mass $M_T \gg m_d$ and charge $Z_T \gg 1$. This latter assumption is made to allow us to neglect the effects of the Coulomb excitation of the target right from the beginning since, for nearly magic nuclei, their lowest excited levels are typically well separated from the ground state. This assumption seems justified, especially for the two scattering systems $d + {}^{208}\text{Pb}$ and $^6\text{He} + {}^{208}\text{Pb}$ we consider in the following, but it is appropriate also for various other targets. For the sake of completeness, in addition, Table I displays the masses and constants that were utilized in the computations in the following.

For the following, moreover, we assume the target nucleus at the origin of the coordinate system and introduce the center-of-mass coordinate $\mathbf{R}$ and the relative position (vector) $\mathbf{r}$ between the core and the halo as

$$\mathbf{R} = \frac{\mu}{m_p}\mathbf{r}_n + \frac{\mu}{m_n}\mathbf{r}_p, \quad \mathbf{r} = \mathbf{r}_n - \mathbf{r}_p, \tag{1}$$

where $\mathbf{r}_n$ and $\mathbf{r}_p$ denote the position vectors of the neutral halo and the charged core, respectively. Figure 1 displays these coordinates, which are appropriate to describe both the polarization as well as a breakup of the projectile during its semiclassical motion along some Coulomb trajectory with given scattering angle θ.

A. Dynamic polarization of the projectile

In the course of the scattering of halo nuclei, as discussed previously [21], the Coulomb field of the target affects the projectile in two different ways while moving along the trajectory. Apart from a polarization of the mass and charge distribution of the halo nucleus, the target field may eventually also cause a breakup of the projectile into its charged core and the neutral halo. Both effects can be taken into account for sufficient low collision energies by applying the adiabatic

TABLE I. Characteristic constants for describing the scattering of deuterons and ^{6}He in the Coulomb field of heavy targets as utilized in the computations in the following.

	ε_0 (MeV)	m_n (amu)	m_p (amu)	m_d (amu)	μ (amu)	Z_p
d	−2.23	1	1	2	1/2	1
^{6}He	−0.975	2	4	6	4/3	2

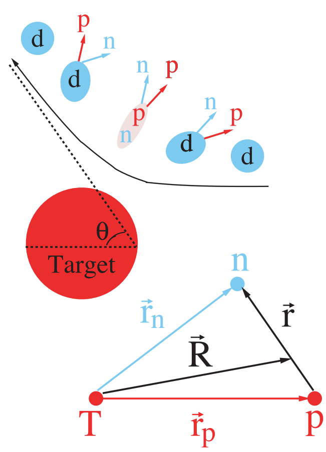

FIG. 1. (Color online) Coordinates to describe the elastic scattering of a halo nucleus in the Coulomb field of a heavy target with charge Z_T and mass $M_T \gg m_d$. The deuteron-like projectile with mass m_d is formed by a charged core p ("proton") and a neutral halo n ("neutron"). See text for further details.

approximation

$$\Psi(\mathbf{r},\mathbf{R}) \approx \chi(\mathbf{R})\,\varphi^{+}(\mathbf{r},\mathbf{R}) \tag{2}$$

and by introducing a dynamic (Coulomb) polarization potential $\delta V(\mathbf{R})$. Indeed, such a potential arises naturally if we assume that the (internal) motion of the halo nucleus is fast compared with the motion of the projectile through the Coulomb field of the target, so that the relative distance between the projectile and target enters the internal motion of the halo nucleus only parametrically.

By making use of this "adiabaticity," it was shown [21] that the Schrödinger equation for the total system,

$$(H_0 - E)\,\Psi(\mathbf{r},\mathbf{R}) = \Delta V(\mathbf{r},\mathbf{R})\Psi(\mathbf{r},\mathbf{R}), \tag{3}$$

can be separated into two (parametrically coupled) equations, one for the center-of-mass motion of the halo nucleus along the Rutherford trajectory, $\chi(\mathbf{R})$, and a second equation,

$$(\hat{T}_{\mathbf{r}} - \Delta V(\mathbf{r},\mathbf{R}) + V_{np}(r))\varphi^{+}(\mathbf{r},\mathbf{R}) = [\varepsilon_0 + \delta V(R)]\varphi^{+}(\mathbf{r},\mathbf{R}), \tag{4}$$

for its relative motion, where the total energy of the halo nucleus $E = E_d + \varepsilon_0$ is the sum of the (asymptotic) kinetic energy E_d and the binding energy ε_0 of the projectile. In these equations, moreover, $\hat{T}_{\mathbf{r}} = -\hbar^2\Delta_{\mathbf{r}}/2\mu$ denotes the kinetic energy (operator) for the relative motion of the neutron halo and the charged core and $V_{np}(r)$ is the (well-known nuclear) Hulthen potential for the deuteron-like halo [27]. The Hulthen potential assumes a special form for the "neutron-proton" interaction with an rather narrow and deep trough. The potential between the target and projectile,

$$\begin{aligned}\Delta V(\mathbf{r},\mathbf{R}) &= Z_p Z_T e^2/R - Z_p Z_T e^2/r_p \\ &= Z_p Z_T e^2[1/R - 1/|\mathbf{R} - \mu/m_p\mathbf{r}|],\end{aligned} \tag{5}$$

includes moreover the deviation from a pure Coulomb field owing to the internal structure of the halo nucleus.

As seen from Eq. (4), the wave function for the relative motion of the projectile, $\varphi^{+}(\mathbf{r},\mathbf{R})$, depends parametrically on the center-of-mass coordinate $\mathbf{R}$ and is associated with the "energy" $[\varepsilon_0 + \delta V(R)]$, in which the binding between the neutron halo and the charged core is modified by the Coulomb field of the target which leads to appear (complex) potential $\delta V(R)$ (with $|\delta V(R)/\varepsilon_0| \ll 1$), to account for the polarization of the projectile by the target. Moreover, by applying the zero-range approximation to the term

$$V_{np}(r)\,\varphi^{+}(\mathbf{r},\mathbf{R}) \approx -\frac{2\pi\hbar^2}{\mu}\left(\frac{\alpha}{2\pi}\right)^{\frac{1}{2}}\delta(\mathbf{r}) \tag{6}$$

it was shown in Ref. [21] that the polarization potential obeys, along with the Coulomb-Green's propagator H_0^{+}, the equation

$$\frac{\mu}{m_p}k(R)\left\{H_0^{+'}(\rho)F_0^{'}(\rho) - \left(\frac{2\eta}{\rho} - 1\right)H_0^{+}(\rho)F_0(\rho)\right\} = -\alpha, \tag{7}$$

where $k(R) = \sqrt{(2m_p^2/\hbar^2\mu)[Z_p Z_T e^2/R + \varepsilon_0 + \delta V(R)]}$ is the wave number of the charged core in the field of the target, $\eta = (m_p^2/\mu)Z_T Z_p e^2/\hbar^2 k(R)$ is the Sommerfeld parameter, and the prime denotes the derivative with respect to $\rho \equiv k(R)R$. Furthermore, the Coulomb-Green's propagator $H_0^{+} = iF_0 + G_0$ is known to consist of the regular Coulomb function [28]

$$F_0(\eta,\rho) = C_0(\eta)\,\rho e^{-i\rho}\,M(1 - i\eta, 2, 2i\rho) \tag{8}$$

at the origin and the irregular Coulomb function

$$G_0(\eta,\rho) = i\,F_0(\eta,\rho) + e^{\frac{\pi\eta}{2} - i\sigma_0}W_{i\eta,1/2}(2i\rho), \tag{9}$$

where, within the definition of these functions, we have

$$C_0(\eta) = e^{-\frac{\pi\eta}{2}}|\Gamma(1 + i\eta)|,$$
$$\exp(i\sigma_0) = \frac{\Gamma(1 + i\eta)}{|\Gamma(1 + i\eta)|}.$$

In these expressions, finally, $M(a,b,z)$ denotes the confluent hypergeometric function of the first kind, $W_{a,b}(z)$ denotes the Whittaker function, and $\Gamma(z)$ denotes the gamma function, respectively. Let us note here that Eq. (7) is free of any additional parameter, apart from those that are needed to describe the energy and impact parameter of the projectile, and may hence be utilized to obtain an (analytic) solution for the elastic scattering of the halo nuclei in the Coulomb field of heavy targets.

B. Analytic expression of the dynamic polarization potential

In our previous work [21], the transcendental equation [Eq. (7)] was solved numerically for every distance R to determine the elastic scattering of ^{6}He + ^{209}Bi at collision energies between 14.7 and 19.1 MeV. Especially Newton's method was applied for solving the complex-valued first-order differential equation [28], which often results in quite tedious computations. In the present work, we now derive an approximate analytical expression for this DPP $\delta V(R)$ by making use of the uniform approximation for the internal motion of the projectile. In this approximation, the Coulomb wave function in Eq. (7) is written in terms of the Airy functions whose argument contains the integral over the Coulomb action. In

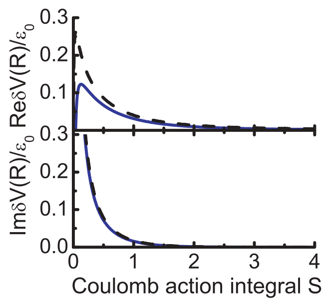

FIG. 2. (Color online) Dynamic polarization potential $\delta V(R)$ as a function of the action integral $S(R,\eta)$ if calculated at the same center-of-mass coordinate R. Results are shown for the exact value of $\delta V(R)$ as obtained from the numerical solution of Eq. (7) for the elastic scattering of ^{6}He + ^{208}Pb (—) and d + ^{208}Pb nuclei (- - -), respectively. The potential is displayed in units of the binding energy of the halo nucleus; the action integral is calculated in units of Planck's constant. See text for further discussions.

more detail, the expression for the Coulomb action integral is defined as

$$S(R,\eta) = \int_{0<\rho<2\eta}^{2\eta} \sqrt{\left(\frac{2\eta}{\rho} - 1\right)}\, d\rho, \qquad (10)$$

with $\rho = k(R)R = \rho[\delta V(R,\eta)]$. However, to make use of this action integral, we first need to know how $S(R,\eta)$ is related to the polarization potential $\delta V(R,\eta)$. This relation can be found if we compute and display both the action integral in Eq. (10) and the polarization potential as functions of the center-of-mass coordinate R, where the $\delta V(R,\eta)$ was obtained from the implicit Eq. (7). Figure 2 displays the polarization potential $\delta V(R)/\varepsilon_0$ for the elastic scattering of ^{6}He + ^{208}Pb and d + ^{208}Pb nuclei as a function of the action integral if calculated for the same value of R. In this figure, the computations were performed for the projectile energies $E_d^{^6\mathrm{He}} = 17.8$ MeV and $E_d^d = 8$ MeV (i.e., just below of the Coulomb barrier). Moreover, the potential is displayed in units of the corresponding binding energies of -0.975 MeV for ^{6}He as observed experimentally [29] and of -2.23 MeV for deuterium [30] (cf. Table I), whereas the action integral is calculated in units of Planck's constant.

Figure 2 demonstrates that the dynamic polarization potentials for the elastic collisions ^{6}He + ^{208}Pb and d + ^{208}Pb are rather close to each other below the Coulomb barrier. Deviations from each other mainly occur for the real part of the polarization potential at small values of S (i.e., in the region of the Coulomb barrier where we cannot neglect nuclear forces). In fact, this independence of the DPP on the particular collision system below and close to the Coulomb barrier enables us to derive an analytical expression for the polarization potential without needing to know the properties of the collision partners in great detail.

To find the dependence of the implicit Eq. (7) on the Coulomb action $S(R,\eta)$, we first need to express this equation in terms of $\delta V(R)$ and ε_0. In practice, this is possible only in an approximate way [since there is no direct dependence between Eq. (7) and the Coulomb action $S(R,\eta)$], for instance, by making use of the criterion

$$\left|\frac{\delta V(R)}{\varepsilon_0}\right| \ll 1 \qquad (11)$$

from the adiabatic model. To rewrite the implicit Eq. (7) in a form that is appropriate for the future analysis of the relation between Eq. (7) and the Coulomb action integral S, let us introduce the function

$$f(R) = 1 - D\left(\frac{2\eta}{\rho} - 1\right)^{-1/2}, \qquad (12)$$

where the expression

$$D = \left(\frac{2\eta}{\rho} - 1\right) H_0^+(\rho)F_0(\rho) - H_0^{+'}(\rho)F_0^{'}(\rho).$$

With this definition at hand, Eq. (7) can be written as

$$\frac{\mu}{m_p}\frac{k(R)}{\alpha}\left(\frac{2\eta}{\rho} - 1\right)^{1/2}\{1 - f(R)\} = 1. \qquad (13)$$

Moreover, using the definition of ρ and the Sommerfeld parameter η from before, we see that their ratio is

$$\frac{2\eta}{\rho} = \frac{Z_p Z_T e^2}{R}\frac{1}{\frac{Z_p Z_T e^2}{R} + \varepsilon_0 + \delta V(R)}, \qquad (14)$$

and by substituting Eq. (14) into Eq. (13) and making use of α and the wave number $k(R)$ of the charged core in the field of the target, we can therefore rewrite the implicit equation for the dynamic Coulomb polarization potential $\delta V(R)$ in the form

$$\sqrt{1 + \frac{\delta V(R)}{\varepsilon_0}}\{1 - f(R)\} = 1. \qquad (15)$$

It is Eq. (15) from which we can easily find the dependence of these equations on the Coulomb action integral. For an adiabatic motion of the projectile for which the criterion of Eq. (11) is satisfied, the function $f(R) \to 0$ if $R \gg R_t$, that is, for all distances far away from the classical Coulomb turning point R_t. To understand how well the function $f(R)$ from Eq. (15) can be approximated by a uniform approximation, Fig. 3 shows the function $f_0 = f\,|_{\delta V=0}$ for the elastic scattering of ^{6}He + ^{208}Pb and for d + ^{208}Pb if expressed in terms of Coulomb action integral [Eq. (10)]. For all values of this integral with $S \geqslant 1/3$, the real part of the function f_0

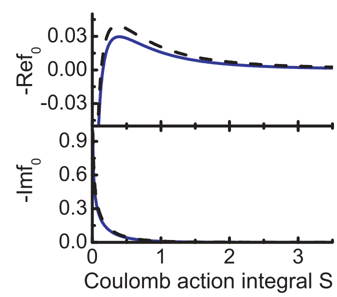

FIG. 3. (Color online) Function $f_0 \equiv f\,|_{\delta V=0}$ for the elastic scattering of ^{6}He + ^{208}Pb (—) and d + ^{208}Pb nuclei (- - -) as functions of the action integral S. The notation is the same as in Fig. 2.

depends very smoothly on S, whereas the imaginary part of f_0 displays an exponential decay for all S with $f_0 \approx 0$ for $S \geqslant 0.5$. This behavior of f_0 therefore shows that the adiabatic approximation also works in the region where the uniform approximation is to be applied for the Coulomb functions in Eq. (12) to obtain an analytical form for $\delta V(R)$.

In the uniform approximation (e.g., for the Sommerfeld parameter $\eta \gg 1$), the regular and irregular Coulomb functions in Eqs. (8) and (9) can be expressed in terms of the Airy functions $Ai(\sigma)$ and $Bi(\sigma)$, respectively [28]. In this approximation, for example, the function $F_0(\eta, \rho)$ is written as [31]

$$F_0(\rho) \simeq \sqrt{\pi}\sigma^{\frac{1}{4}} \left(\frac{2\eta}{\rho} - 1\right)^{-\frac{1}{4}} Ai(\sigma), \tag{16}$$

while its derivative becomes

$$F_0^{'}(\rho) \simeq \left(\frac{2\eta}{\rho} - 1\right)^{\frac{1}{2}} [1 - a(\sigma) + h(\rho)]\, F_0(\rho), \tag{17}$$

and where we have utilized the short-hand notation

$$a(\sigma) = 1 + \frac{Ai^{'}(\sigma)}{\sigma^{\frac{1}{2}} Ai(\sigma)} + \frac{1}{4\sigma^{\frac{3}{2}}},$$

$$h(\rho) = \frac{1}{8\eta}\left(\frac{2\eta}{\rho}\right)^2 \left(\frac{2\eta}{\rho} - 1\right)^{-\frac{3}{2}}, \tag{18}$$

$$\sigma = \left(\frac{3}{2}S\right)^{\frac{2}{3}}.$$

Similarly, the irregular Coulomb function $G_0(\eta, \rho)$ in Eq. (9) is given in the uniform approximation by [31]

$$G_0(\rho) \simeq \sqrt{\pi}\sigma^{\frac{1}{4}} \left(\frac{2\eta}{\rho} - 1\right)^{-\frac{1}{4}} Bi(\sigma), \tag{19}$$

with the derivative

$$G_0^{'}(\rho) \simeq -\left(\frac{2\eta}{\rho} - 1\right)^{\frac{1}{2}} [1 - g(\sigma) - h(\rho)]\, G_0(\rho), \tag{20}$$

and with

$$g(\sigma) = 1 - \frac{Bi^{'}(\sigma)}{\sigma^{\frac{1}{2}} Bi(\sigma)} - \frac{1}{4\sigma^{\frac{3}{2}}}.$$

With these expressions substituted into the differential equation (15), indeed, an (approximate) solution is much simpler to obtain than for the exact equation. Following the work of Berry and Mount [31], we have that the uniform approximation to the Coulomb functions is valid for

$$\epsilon(\rho) = \left| \left(\frac{2\eta}{\rho} - 1\right)^{-1} \left(\frac{d\sigma}{d\rho}\right)^{\frac{1}{2}} \frac{d^2}{d\rho^2} \left(\frac{d\sigma}{d\rho}\right)^{-\frac{1}{2}} \right| \ll 1, \tag{21}$$

Figure 4 displays the value $\epsilon[\rho(R)]$ as a function of the center-of-mass coordinate R for the elastic scattering of ^{6}He + ^{208}Pb and for $d + {}^{208}$Pb, respectively. As seen from this figure, the uniform approximation [Eqs. (16)–(20)] of the Coulomb functions is useful and appropriate for all values R of the center-of-mass coordinate, including even the region around the classical turning points at $R_t^d \approx 10$ fm and $R_t^{^6\mathrm{He}} \approx 15$ fm, respectively. Note that Eqs. (16)–(20) are very similar also to the quasiclassical expressions for the Coulomb functions in Ref. [28].

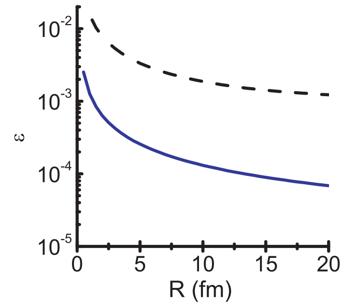

FIG. 4. (Color online) The criterion of Eq. (21) as a function of the center-of-mass coordinate R. Results are shown for the elastic scattering of ^{6}He + ^{208}Pb (—) and for $d + {}^{208}$Pb nuclei (- - -).

Now, let us return to the DPP $\delta V(R)$. If we expand the left-hand side of Eq. (15) in powers of the small parameter $\delta V(R)/\varepsilon_0$ up to first order, we obtain

$$\left(1 + \frac{\delta V(R)}{2\varepsilon_0}\right) = 1 - \mathrm{Re}\, f(R) - i\, \mathrm{Im}\, f(R). \tag{22}$$

From this expression, we can construct $\mathrm{Re}\, f(R)$ and $\mathrm{Im}\, f(R) \cdot \exp(2S)$ by using Eqs. (16)–(20), and both functions are found to behave smoothly with regard to the Coulomb action (variable) S. Because of this smooth behavior and since the adiabatic criterion [Eq. (11)] applies for (almost) all R, we finally obtain

$$\mathrm{Re}\, f(R) = \mathrm{Re}\, f(R)|_{\delta V=0} \simeq \mathrm{Re}\, f_0(R), \tag{23}$$

$$\mathrm{Im}\, f(R) \simeq \mathrm{Im}\, f_0(R) - 2\mathrm{Im}\, f_0(R) \left(\frac{dS}{d\delta V(R)}\right)_{\delta V=0} \delta V(R). \tag{24}$$

By substituting Eqs. (23) and (24) into Eq. (22), the DPP takes the form

$$\delta V(R) \simeq 2\varepsilon_0 \frac{\mathrm{Re}\, f_0(R) + i\, \mathrm{Im}\, f_0(R)}{1 + 2i S_0^{'} \varepsilon_0 \mathrm{Im}\, f_0(R)}, \tag{25}$$

where $S_0 = S\,|_{\delta V=0}$ and the derivative of the Coulomb action integral with respect to the DPP at the point $\delta V = 0$ is given by

$$S_0^{'} = 2\left(\frac{dS}{d\delta V(R)}\right)_{\delta V=0} = \frac{1}{\frac{Z_p Z_T e^2}{R}} \frac{2\eta}{\rho} \left(S_0 + 2\rho\sqrt{\frac{2\eta}{\rho} - 1}\right). \tag{26}$$

This (analytical) approximate expression for the DPP is the main result of this work; this expression can be utilized if the neutron halo nucleus (or the deuteron) follows adiabatically a Rutherford trajectory within a strong Coulomb field. Let us emphasize here that this DPP has been obtained without any multipole expansion of the projectile-target interaction.

The expression for the polarization potential [Eq. (25)] has been utilized to calculate the elastic scattering of both the deuteron and ^{6}He on ^{208}Pb nuclei as functions of the projectile-target separation R. In Fig. 5, we display the real and imaginary

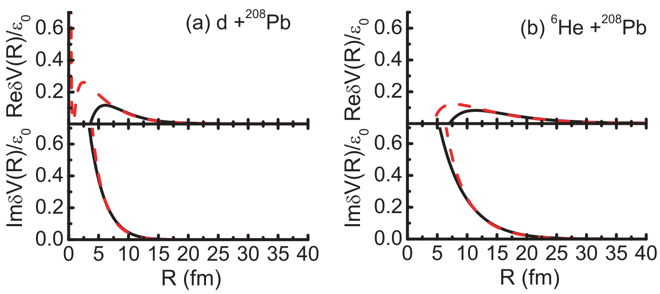

FIG. 5. (Color online) Dynamic polarization potential $\delta V(R)$ as functions of the projectile-target separation R. Comparison is made between the (numerically) exact value $\delta V(R)$ (—) from the implicit Eq. (15) and the approximate analytical expression [Eq. (25)]. Results are shown for (a) the scattering of $d + {}^{208}$Pb at the collision energy $E_d^d = 8$ MeV and for (b) ^{6}He + ^{208}Pb at the energy $E_d^{^6\mathrm{He}} = 17.8$ MeV. All potentials are displayed in units of the binding energy of the corresponding projectile.

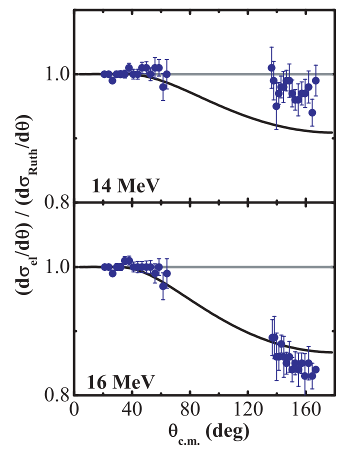

FIG. 6. (Color online) Elastic angle-differential cross sections for the collision of low-energy ^{6}He + ^{208}Pb nuclei as a function of the scattering angle θ in the center-of-mass frame. The cross sections are taken relative to the cross sections of pure Rutherford scattering for a projectile with mass m_d and charge Z_p and are shown for two collision energies as observed experimentally [15].

parts of this potential in units of binding energy of the corresponding projectiles. In both cases, the calculations were performed just below of the Coulomb barrier (i.e., at $E_d^d =$ 8 MeV and $E_d^{^6\mathrm{He}} = 17.8$ MeV, respectively). Comparison is made in this figure between the—numerically—exact value (solid line) from Eq. (15) and the approximate analytical expression (dashed line) for $\delta V(R)$ from Eq. (25). Note that both approximations for the polarization potential coincide for all $R > R_t$ larger than the classical Coulomb turning points, which are $R_t^d = 8$ fm for $d + {}^{208}$Pb and $R_t^{^6\mathrm{He}} = 15$ fm for ^{6}He + ^{208}Pb, respectively. For similar reasons, we also have a very good agreement for the Coulomb action integral $S \geqslant 1/3$ between its numerical and analytical treatment at $R > R_t$. However, although the modulus of the potential is small, the real and imaginary parts of the polarization potential show a long-range behavior. It is this behavior of the interaction potential between a deuteron-like nucleus and a heavy target that may be one of the causes for the rather large and atypical (radii and diffuseness) parameters of the optical potential in the scattering treatment of Ref. [13]. Let us note, moreover, that the DPP in our computations was obtained by taking into account only the Coulomb interaction between the target and the projectile. As shown in Ref. [15], however, there might be other sources that contribute to the DPP apart from the Coulomb interaction between ^{6}He and ^{208}Pb. Further theoretical analysis will be required to better understand all the physical reasons that may affect the DPP in the scattering of halo nuclei.

III. CALCULATION OF THE ELASTIC CROSS SECTIONS FOR ^{6}He

Using the analytic expression for the DPP [Eq. (25)], we can predict the theoretical cross sections for the elastic scattering of ^{6}He + ^{208}Pb at energies below and close to the Coulomb barrier (~20 MeV). For this, we apply $\delta V(R)$ as an optical potential (without any need of introducing additional parameters) and calculate the differential cross section for the elastic scattering of a ^{6}He under the assumption that the ^{6}He nucleus consists of a α-like core and a dineutron halo. Figure 6 displays the (ratio of the) cross sections $(d\sigma_{\mathrm{el}}/d\theta)/(d\sigma_{\mathrm{Ruth}}/d\theta)$ for the elastic scattering of ^{6}He + ^{208}Pb target nuclei as a function of the scattering angle, relative to the cross section for pure Rutherford scattering of the projectile with mass m_d and charge Z_p. In this figure, the Rutherford cross section therefore appears as a straight (constant) line. For the two projectile energies $E_d = 14$ and 16 MeV, which are just below of the Coulomb barrier, our predictions for the differential cross sections are compared also with the recent measurement by Sanchez-Benitez *et al.* [15] for which the ^{6}He beam was produced by the Cyclotron at the Centre de Recherches du Cyclotron at Louvain-la-Neuve, Belgium [32].

Deviations from a purely Rutherford cross section occur for several reasons: Although, at small angles, these deviations can be explained by the so-called electric polarization of the projectile [33], the decrease at larger angles (in the backscattering) mainly arise from the Coulomb breakup of the ^{6}He halo nuclei, which increases because of the strong Coulomb field. Overall a very good agreement is found between our theoretical predictions and the experiments, in particular at small angles ($\theta_{\mathrm{c.m.}} = 20°$–$64°$). A slight overestimation of the cross section occurs at the energy $E_d^{^6\mathrm{He}} = 14$ MeV for large angles, which means that the probability for a breakup of ^{6}He is somewhat smaller at this energy than described by the DPP δV. However, the measured cross sections are slightly underestimated at large scattering angles for $E_d^{^6\mathrm{He}} = 16$ MeV. This underestimation relates perhaps to the nuclear interaction between target and projectile. In the future, we therefore plan to include an additional bare interaction that accounts for these nuclear effects.

IV. CONCLUSIONS

In summary, the elastic scattering of deuteron and light halo nuclei in the (Coulomb) field of heavy targets has been investigated for collision energies below and close to the

Coulomb barrier. By assuming an adiabatic approach for the internal halo-core motion of the projectile along a classical Rutherford trajectory, emphasis was placed on deriving an analytical expression for the (dynamic) polarization potential. Apart from the elastic scattering of the projectiles, this potential enables one to describe the internal dynamics of the halo nucleus, including its (electrical) polarization and breakup. The dynamic polarization potential can be applied for any arbitrary system with a dineutron configuration. For a strong enough Coulomb field, this potential may describe also the breakup of the "deuteron-like" projectile into its neutron and proton parts. In particular, it has been shown that the asymmetry of the halo nuclei leads to a considerable decrease in the (elastic) scattering cross section at large scattering angles.

To derive the dynamic polarization potential, we utilized the uniform approximation for the Coulomb functions apart from the adiabatic motion of the projectiles along their trajectory. The obtained expression shows a long-range behavior for the dynamic polarization potential, although the modulus of both its real and imaginary part is small. This long-range behavior of the potential is expected to be the main reason for the rather large (and atypical) diffuseness parameter that occurs in the optical potential for elastic scattering [13]. But further theoretical analysis is likely required to understand all sources of the DPP. Detailed computations have been carried out in this work for the elastic scattering of $d + {}^{208}$Pb and ^{6}He + ^{208}Pb at collisions energies of 8 and 17.8 MeV, respectively. The theoretical cross sections predicted from the model agree well with the measurements by Sanchez-Benitez and co-workers (cf. Fig. 6) and, hence, make a dineutron configuration very likely for the ground state of the ^{6}He halo nucleus. No additional parameters were needed to explain the deviations from the Rutherford cross section.

ACKNOWLEDGMENT

This work has been supported by the GSI under Project No. KS-FRT.

[1] I. Tanihata *et al.*, Phys. Rev. Lett. **55**, 2676 (1985).
[2] J. S. Al-Khalili, J. A. Tostevin, and I. J. Thompson, Phys. Rev. C **54**, 1843 (1996).
[3] N. Keeley and N. Alamanos, Phys. Rev. C **77**, 054602 (2008).
[4] P. G. Hansen and B. Jonson, Europhys. Lett. **4**, 409 (1987).
[5] Yu. Ts. Oganessian, V. I. Zagrebaev, and J. S. Vaagen, Phys. Rev. C **60**, 044605 (1999).
[6] J. C. Pacheco and N. Vinh Mau, Phys. Rev. C **65**, 044004 (2002).
[7] N. Michel, W. Nazarewicz, and M. Ploszajczak, Phys. Rev. C **75**, 031301(R) (2007).
[8] W. Liu *et al.*, Nucl. Phys. **A758**, 110 (2005).
[9] C. A. Bertulani, Phys. Rev. Lett. **94**, 072701 (2005).
[10] J. S. Al-Khalili and J. A. Tostevin, Phys. Rev. Lett. **76**, 3903 (1996).
[11] G. Baur, K. Hencken, and D. Trautmann, Prog. Part. Nucl. Phys. **51**, 487 (2003).
[12] G. Baur and S. Typel, Prog. Part. Nucl. Phys. **59**, 122 (2007).
[13] E. F. Aguilera *et al.*, Phys. Rev. C **63**, 061603(R) (2001).
[14] A. M. Sanchez-Benitez *et al.*, J. Phys. G **31**, S1953 (2005).
[15] A. M. Sanchez-Benitez *et al.*, Nucl. Phys. **A803**, 30 (2008).
[16] M. Yahiro, M. Nakano, Y. Iseri, and M. Kamimura, Prog. Theor. Phys. **67**, 1467 (1982).
[17] N. Austern, Y. Iseri, M. Kamimura, M. Kawai, G. Rawitscher, and M. Yahiro, Phys. Rep. **154**, 125 (1987).
[18] T. Matsumoto, T. Egami, K. Ogata, Y. Iseri, M. Kamimura, and M. Yahiro, Phys. Rev. C **73**, 051602(R) (2006).
[19] T. Egami, K. Ogata, T. Matsumoto, Y. Iseri, M. Kamimura, and M. Yahiro, Phys. Rev. C **70**, 047604 (2004).
[20] L. F. Canto, R. Donangelo, P. Lotti, and M. S. Hussein, Phys. Rev. C **52**, R2848 (1995).
[21] L. Borowska, K. Terenetsky, V. Verbitsky, and S. Fritzsche, Phys. Rev. C **76**, 034606 (2007).
[22] M. V. Andres, J. Gomez-Camacho, and M. A. Nagarajan, Nucl. Phys. **A579**, 273 (1994).
[23] K. Rusek, N. Keeley, K. W. Kemper, and R. Raabe, Phys. Rev. C **67**, 041604(R) (2003).
[24] D. Sackett *et al.*, Phys. Rev. C **48**, 118 (1993).
[25] J. J. Kolata *et al.*, Phys. Rev. Lett. **81**, 4580 (1998).
[26] A. M. Moro, K. Rusek, J. M. Arias, J. Gomez-Camacho, and M. Rodriguez-Gallardo, Phys. Rev. C **75**, 064607 (2007).
[27] G. Baur and D. Trautmann, Nucl. Phys. **A191**, 321 (1972).
[28] *Handbook of Mathematical Functions*, 8th ed., edited by M. Abramowitz and I. A. Stegun (Dover, New York, 1972).
[29] J. Wang *et al.*, Phys. Rev. C **65**, 034306 (2002).
[30] R. Bell and L. Elliott, Phys. Rev. **79**, 282 (1950).
[31] M. Berry and K. Mount, Rep. Prog. Phys. **35**, 315 (1972).
[32] J. Vervier, Nucl. Phys. **A616**, 97 (1997).
[33] T. L. Abelishvili and A. G. Sitenko, Ukr. Fiz. Zh. **6**, 3 (1961).